

The behaviour of point charges in dielectric media

Piet Th. van Duijnen,^a Hilde D. de Gier,^a Ria Broer,^a Remco W.A. Havenith^{a,b,c,*}

^a*Theoretical Chemistry, Zernike Institute for Advanced Materials, University of Groningen, Nijenborgh 4, 9747 AG Groningen, The Netherlands, e-mail: r.w.a.havenith@rug.nl*

^b*Stratingh Institute for Chemistry, University of Groningen, Nijenborgh 4, 9747 AG Groningen, The Netherlands*

^c*Ghent Quantum Chemistry Group, Department of Inorganic and Physical Chemistry, Ghent University, Krijgslaan 281 – (S3), B-9000 Gent, Belgium*

Abstract:

Screened Coulomb interaction in dielectrics is often used as an argument for a lower exciton binding energy and easier exciton dissociation in a high dielectric material. In this paper, we show that at the length scales of excitons, the screened Coulomb law is invalid and a microscopic (quantum chemical) description is necessary to describe the exciton dissociation process. The screened Coulomb law is only valid in regions where the electron and hole are further separated than a few Ångströms or a few tens of Ångströms. This is illustrated here for charges in different environments.

Keywords: Organic photovoltaics, dielectric constant, screened Coulomb law, exciton binding energy, computational chemistry

1. Introduction.

In the quest for more efficient organic photovoltaic devices (OPVs), the use of materials with a high dielectric constant has been suggested.[1] One reason why organic photovoltaic systems are less efficient than inorganic solar cells like those based on silicon, is the high exciton binding energy. This is commonly attributed to the low dielectric constant of OPVs ($\epsilon \approx 4$).[2, 3] This idea is based on the screened Coulomb law in ponderable materials, which tells us that the interaction energy and force between point charges embedded in such media are given by, respectively (in atomic units),

$$\begin{aligned} U_{ij} &= Q_i Q_j / \epsilon R_{ij} \\ \mathbf{F}_{ij} &= Q_i Q_j (\mathbf{R}_j - \mathbf{R}_i) / \epsilon R_{ij}^3 ; \epsilon \geq 1.0 \end{aligned} \quad (1)$$

with Q_i and Q_j the point charges, \mathbf{R}_i and \mathbf{R}_j their positions, R_{ij} the distance between them and ϵ the (relative) dielectric constant of the medium. By definition, $\epsilon \geq 1.0$, furthermore, ϵ is independent of the type (plus or minus) of the charges, which means that like (+/+, or -/-) and unlike (+/-) interactions are equally reduced as compared to the vacuum situation ($\epsilon = 1.0$). The proof is simple: a charge Q_i in a cavity with radius a , embedded in an infinite continuum with dielectric constant ϵ gives rise to an induced charge on the cavity's surface (Gauss' law):

$$Q_i^* = -\left(1 - \frac{1}{\epsilon}\right)Q_i \quad (2)$$

which is independent of a . Letting a going to zero, the potential at \mathbf{R}_i vanishes and one has effectively two coinciding, non-interacting point charges. When a second charge (Q_j) is introduced, that charge gives only rise to a similar pair of charges if the

polarisation of the medium at R_j is not affected by the presence of Q_i . In that case the distance R_{ij} is so large that the total interaction energy can be written as[4]

$$U_{ij} = \frac{1}{R_{ij}} \left[Q_i Q_j + \frac{1}{2} (Q_i^* Q_j + Q_i Q_j^*) \right] \quad (3)$$

which, after inserting Eq. (2), gives Eq. (1).

Hence, Eq. (1) holds only for *macroscopic* situations, *i.e.*, the charges are averages over macroscopic volumes, although small with respect to the actual size of the system, and therefore should be at *macroscopic* distances (at least about 100 Å[5]) from each other. Moreover, they should also be at macroscopic distances from any boundary for the system characterized with ϵ . However, an exciton generated in OPV materials consists of a pair of unlike charges at a separation of 10 - 20 Å in a molecular, and therefore highly anisotropic, polarisable environment. As a consequence, Eq. (1) should not be used to describe or explain charge separation: the charges must already be farther separated before the screened Coulomb law is applicable. Hence, it is not straightforward that the charges involved in an exciton behave like they were in a macroscopic dielectric, and a more indepth consideration of their behaviour is necessary to understand charge separation in OPVs better.

As early as 1982, Van Duijnen and Thole[6] noted that a dielectric placed *between* two interacting charges increases the interaction ($\epsilon_{eff} < 1.0$). Later, Rullmann *et al.*[7] showed that microscopic collections of (point) charges and polarisabilities show behaviour that cannot be described by the simple expression of Eq. (1), and in 1993 De Vries and Van Duijnen[8] pointed out some of the problems connected with mixing macroscopic and (quantum mechanical) microscopic descriptions of the behaviour of charges. In 1995 Van Duijnen and De Vries[9] studied systematically assemblies of point charges and polarisabilities, and found that the ‘effective’

dielectric constants (ϵ_{eff} , obtained as the ratio of the forces *in vacuo* and in *microscopic* assemblies) may be different for like and unlike interactions. This deviation was observed to the extent that some arrangements lead to $\epsilon_{eff} < 1.0$ (*i.e.*, unlike charges attract each other more than in vacuum) and even $\epsilon_{eff} < 0.0$ (*i.e.*, like charges attract each other). Other examples of this unexpected behaviour of like charges can also be found in works of Jarque[10] and Zangi.[11] The ‘unexpected’ in the preceding sentence holds only in ‘dielectric’ terms: these results are obtained from microscopic descriptions where the dielectric constant, as a macroscopic parameter, is not appropriate. Thus for excitons, behaviour that deviates from Eq. (1) is also expected, and this is the subject of the present investigation. Interestingly, Deslippe *et al.*[12] reported exciton interactions in carbon nanotubes and found interactions to be larger than ‘bare’ interactions, which they coined ‘anti-screening’.

In a theoretical study on excitons in polymers by Van der Horst *et al.*[13] applying the Bethe-Salpeter equation, exciton binding energies were found of 0.4 - 0.6 eV. Here, layers perpendicular to the polymer chain were modelled with a dielectric continuum with $\epsilon_{\perp} = 3.0$. In an appendix, the authors explain how they arrive at the actual used value of ϵ_{\perp} by considering the Poisson equation. The operator for the electron repulsion energies they used is:

$$W(\mathbf{r}, \mathbf{r}') = W_{\epsilon}(|\mathbf{r} - \mathbf{r}'|) = 1 / (\epsilon |\mathbf{r} - \mathbf{r}'|) \quad (4)$$

i.e., they divided the interaction by the dielectric constant. This means that the continuum is supposed to be present everywhere as a sort of ether. Their procedure leads to exciton binding energies of 0.4 - 0.6 eV, corresponding to interaction *distances* of 8 – 12 Å. Also Lethonen *et al.*[14] use the bulk dielectric constant for screening Coulomb interactions in their computational studies based on an effective mass model on quantum dots with diameters up to only 7 nm.

A much repeated picture is that of a Coulomb potential like Eq. (1) with indications of the interaction between charges in a dielectricum. Gregg and Hanna[15] suggest that the strong interaction in excitons is caused by the small dielectric constant in typical OPVs ($\epsilon \approx 4$), in contrast with the free electron-hole pairs in inorganic semiconductors ($\epsilon \approx 15$). In 2004, Gregg *et al.*[16] put this even stronger: “Thus, increasing ϵ ... leads to a greater average distance between the charges.” But there is also a warning: “Finally, ϵ is a bulk quantity and is valid only over distances of many lattice spacings; ...” In following papers, this warning is absent, and in the recent review of Clarke and Durrant[2] the dielectric constant is still a very important parameter, and the Onsager model, or more recently developed versions[17-22] of it, is still the main[1] operative theory.[23] In all these works the expected effect of the dielectric constant (or the permittivity) comes from model calculations based on the Onsager model.

However, excitons in OPVs require a microscopic description, *i.e.*, all local interactions should be taken into account. In this contribution, the effective force between charges is studied in different materials, and the consequences for OPVs are discussed. We will demonstrate that the screened Coulomb law is not applicable for the description of an arbitrary collection of charges and polarisabilities.

2. Dielectric or not?

Recently Van Duijnen and Swart reported a Discrete Reaction Field (DRF)[24] study on Si_n -clusters[25] (n ranging from 3 to ~ 5000) in which they arrived at the experimental dielectric constant from first principles for the larger clusters ($n = 1750, 4950$).

In the DRF-method the many-body polarisation is treated correctly:

$$\mu_p = \alpha_p [E_p^0 + \sum_{q \neq p} t_{pq} \mu_q] \quad (5)$$

In Eq. (5), μ_p is the dipole induced at position p by the field E^0 plus the field of all other induced dipoles. E^0 consists of any applied field plus the field of any charge distribution in the system. The dipole-dipole interaction tensors t_{pq} in Eq. (5) contain only geometric parameters. In DRF, the interactions are properly damped at short distances in order to avoid too large and unphysical results.[26, 27] The electric potentials, fields and field gradients of charges are damped in a consistent way and the damped fields and dipole-dipole tensors are the derivatives of the potential and the field, respectively [24]. For an arbitrary collection of charges and polarisabilities, Eq. (5) leads to a matrix equation:

$$\mathbf{M} = \mathbf{B}\mathbf{E}^0 = [\mathbf{A}^{-1} - \mathbf{T}]^{-1} \mathbf{E}^0 \quad (6)$$

in which \mathbf{M} is the vector of (self-consistent) induced dipoles, \mathbf{E}^0 the vector of the initial field, \mathbf{A} the block-diagonal matrix of the (vacuum) polarisabilities, and \mathbf{T} the (off-diagonal) interaction tensors. Hence, \mathbf{B} is a normal (but many-body) polarisability thus leading to an induction energy:

$$U_{ind} = -\frac{1}{2} \mathbf{E}^0 \mathbf{B} \mathbf{E}^0 \quad (7)$$

By applying unit fields in x -, y - and z -directions, the *effective* mean polarisabilities are obtained from Eq. (6). We note here that the \mathbf{T} -blocks in the condensed phases generally lead to effective local polarisabilities that are *smaller* than the vacuum values.[25]

Reversely, by fitting Eq. (6) to (experimental or calculated) molecular polarisabilities, the vacuum, or ‘free-atom’ polarisabilities $\{\alpha_p\}$ are obtained. With these (‘input’) parameters the polarisabilities of molecules – not belonging to the learning sets – are calculated from Eq. (6) with experimental accuracy.[28] Typically, each ‘free’ atomic

polarisability is independent of its ‘chemical environment’: the latter is in all cases absorbed in the **T**-blocks of **B**.

In Fig. 1, the average (per atom) mean polarisabilities of atoms of n -clusters ($n = 4950$) of carbon and silicon in their experimental (diamond) structures are plotted as a function of their distance to the centre of the (roughly spherical) clusters. For silicon, the ‘free atom’ polarisability ($\alpha_{\text{Si}} = 5.9 \text{ \AA}^3$) was obtained from the calculated polarisability[29] of Si_3 , while for carbon the default value in DRF90 was used ($\alpha_{\text{C}} = 1.3 \text{ \AA}^3$), which came from a fit to a learning set of 52 molecules.[27]

Figure 1

We note that the calculated average atomic polarisability in the interior is substantially smaller than the input value. This is caused by the local field contributions of the induced dipoles in the environment. Since there are no induced counteracting dipoles outside the edge of the clusters, the mean polarisabilities there are larger. For Si, $\alpha^{\text{eff}} = 3.72 \text{ \AA}^3$ is in perfect agreement with the value obtained from the Clausius-Mossotti relation:

$$\alpha = \frac{3}{4\pi} \frac{\epsilon - 1}{\epsilon + 2} \Omega = \frac{\epsilon - 1}{\epsilon + 2} \langle r \rangle^3 \quad (8)$$

where Ω is the average atomic volume, $\langle r \rangle$ the average atomic radius, and ϵ the dielectric constant. Note, that the reverse relation

$$\epsilon = \frac{2\alpha + \langle r \rangle^3}{\langle r \rangle^3 - \alpha} \quad (9)$$

is more error prone than Eq. (8), because the denominator comes from numbers that are in general nearly equal. The average atomic radii were obtained from the volumes of spheres where the average atomic polarisabilities were about constant (Si: 20 \AA ,

1700 atoms; C: 14 Å, 1900 atoms). From the simulations, $\epsilon_{\text{Si}} = 12$ and $\epsilon_{\text{C}} = 6$ were found, for which the experimental values are, respectively, 11.8 and 5.5. That the error in ϵ_{C} is slightly larger than in ϵ_{Si} , is in agreement with the fact that α_{Si} came from a specific fit which in general predicts polarisabilities within about 1%, while α_{C} was taken from a fit to a collection of different molecular polarisabilities[27] which predicts molecular polarisabilities with an error of about 6%.

Although the calculated dielectric constants are in good agreement with experiment, the question is whether these clusters behave as real dielectrics. In order to check this, the force between two charged atoms (each with $|Q| = 1$ au), about 46 Å apart in the Si_{4950} cluster was calculated from finite differences (Table 1). The results show that the forces for like and unlike charges scale differently, and that the effective dielectric constant is far from $\epsilon = 12$: this cluster cannot be described as a dielectric continuum.

Table 1

3. A model exciton in a donor-acceptor complex

In Fig. 2, we present a typical molecular donor-acceptor complex. First, we prepared a point charge model of the donor-acceptor complex (**1**, Fig. 2) from INDO-SCF[30] calculations. Next, we simulated – crudely – an exciton by putting charges in the centres of mass of the donor and the acceptor moieties, respectively, and computed with DRF90 the electrostatic and induction interaction energies, and the forces between them by finite differences (Tables 2 and S2). The short-range repulsion was neglected here, because the approximation used in DRF90 is not valid for this intra-

molecular region. We used the default polarisabilities of DRF90 for the atoms of the complex while the ‘excitonic’ point charges were treated as ‘hydrogen’ atoms with a default polarisability of about 0.5 \AA^3 .

Figure 2 and Table 2

The (damped) coulombic force between the ‘excitonic’ point charges embedded in **1** is repulsive, due to the presence of the ground state charges and polarisabilities of **1**. The induction contribution is of about the same size and is repulsive, too.

Figure 3

Next, we extended the environment by immersing **1** in C_{4950} and Si_{4950} , respectively, in which the atoms of the clusters that were too close to the atoms of complex **1** were deleted (see Fig. 3 and Table 2). Because the C and Si atoms are not charged, and the atoms surrounding **1** are relatively large, the electrostatic contributions to the forces are the same as before, while the induction now comes from all charges, and the interactions between all induced dipoles in the system. First, we learn from Table 2 that extending the environment of the system has little effect: the total forces between the ‘excitonic’ point charges in the clusters are of the same order as those in ‘vacuum’. This indicates that the immediate (molecular) environment is more important than the embedding clusters. Moreover, the effect is counterintuitive in the sense that one expects a reduction of the interactions, while in fact the forces increase in the clusters. The forces in carbon and silicon are almost equal while the dielectric constants of the clusters differ by a factor of two (see “Dielectric or not?”)! The

effective dielectric constants, obtained as the ratio between the total forces *in vacuo* and those in the clusters, do not relate to the macroscopic dielectric constant.

Finally, only the two ‘excitonic’ point charges were ‘solvated’ in a similar way for further investigating the dielectric behaviour of the clusters. From these last experiments we obtained the effective dielectric constants for C and Si, which clearly deviate considerably from the numbers in the preceding section. Moreover, repeating this for *like* charges (+/+), the ϵ_{eff} differ from those for the unlike (+/-) charges, showing that even these clusters of more than 4500 atoms do not behave as proper dielectrics, or rather, the interactions cannot be described in terms of the screened Coulomb law of Eq. (1). This is caused mainly by the too small distance between the charges: in order to satisfy Eq. (1), the charges should be so far apart that induction effects due to one of them vanishes around the other one.

4. Modelling exciton dissociation in different materials

In the preceding sections we treated two point charges at specific geometries and different distances. In this section, the dissociation of two oppositely charged point particles ($Q = \pm 1$ au) is studied in a rectangular box ($a = 20 \text{ \AA}$, $b = 20 \text{ \AA}$, $c = 40 \text{ \AA}$) filled with nonane (**2**, 82 molecules, $\rho = 1.09 \text{ g/ml}$), 1-methoxy-2-(2-methoxyethoxy)ethane (**3**, 78 molecules, $\rho = 1.09 \text{ g/ml}$), and with 1,8-diiodooctane (**4**, 48 molecules, $\rho = 1.82 \text{ g/ml}$), respectively. The distance between the charges was varied between 2 \AA and 30 \AA in the c -direction, and the force between the charges was calculated by numerical differentiation (at each distance, the molecules in the box were allowed to relax (MM3 force field [31])). After relaxation, the molecules in the box were treated both fully quantum mechanically (HF/6-31G) and using the DRF

force field (GAMESS-UK [32]). The force as a function of the distance is plotted in Fig. 4.

Figure 4

It is evident from Fig. 4, that these clusters of molecules do not behave like dielectric media. The forces between the charges do not vary smoothly with distance and they deviate considerably from Eq. (1). A comparison between the HF and DRF calculated forces shows for both methods similar trends, the DRF curve is however more extreme in the deviations from ideal behaviour, because the DRF response is basically linear, while for electrons at short distances the response is nonlinear. In all three media regions exist where the charges attract each other more than in vacuum and regions where they even repel each other. At very short distances ($< 5 \text{ \AA}$), the Coulombic force between the two charges is effectively reduced by the presence of the medium, but no dielectric *constant* emerges. At intermediate distances ($10 - 25 \text{ \AA}$), **3** seems to favour exciton dissociation. The other compounds, **2** and **4**, show the same behaviour, but at longer distances ($> 25 \text{ \AA}$). Compound **3** shows at these distances attraction of the charges again. However, the irregular shape of the curves is presumably very dependent on the orientation of the molecules surrounding the charges, thus conclusions regarding which medium would enhance exciton dissociation cannot be drawn from this study. What is shown by this model study is that for distances of $2 - 30 \text{ \AA}$ between charges no unique dielectric can be defined, and exciton dissociation has to be studied using microscopic (quantum chemical) methods.

5. Efficiency and permittivity in practice

Recently, a study was reported in which it was found that the OPV efficiency was enhanced by a larger dielectric constant.[33] It is argued that the exciton binding energy was lowered by increasing the permittivity of thin films of B,O-chelated azadipyrromethene (BO-ADPM) blended with camphoric anhydride (CA). The authors measured an increased internal quantum efficiency of ~30%, related to an increase of the dielectric constant from ~4.5 to ~11. In the light of the findings presented here, a more elaborate explanation than that based on Eq. (1) must be given to rationalise their results, because the hole-electron distance is far too small to be affected by the dielectric medium. Furthermore, only tiny changes in the absorption spectrum in the various mixtures are observed, suggesting that the interaction between BO-ADPM and CA is very weak. To confirm these experimental findings, we performed a number of INDOs/DRF/CIS[25] calculations, with the standard INDOs parameterization,[30] on BO-ADPM properties. The experimental spectrum consists of bands around 325, 500 and 750 nm (3.8, 2.5 and 1.6 eV).

The ground state vacuum dipole moment of BO-ADPM was found to be 1.31 Debye (0.51 au) and we applied the Born formula to get a first estimate of the solvation energy for a collection of multipoles in a spherical cavity with radius r :

$$\Delta G_{solv} = -\frac{1}{2} \sum_l \sum_{m=-l}^l r^{-(2l+1)} \frac{[(l+1)(\epsilon-1)]}{[l+\epsilon(l+1)]} \langle T_{lm} \rangle^2 \quad (10)$$

For a hole-electron dipole of 0.51 au in a sphere with $r = 22$ Bohr, *i.e.*, a sphere just containing the BO-ADPM molecule, placed in a continuum with $\epsilon = 11$, we get $G_{solv} \approx -1.1 \cdot 10^{-5}$ Hartree ($-3 \cdot 10^{-4}$ eV).

Considering the Born formula to be a too crude approximation, we used the DRF90 suite and applied INDOs/DRF/CIS[25] for QM/MM to calculate the spectrum of BO-ADPM in a sphere of the same size and calculated the interaction with the continuum and the absorption spectrum, using the standard INDOs parameterization. The calculated spectrum (red curve in Fig. 5) was very similar to the experimental one, apart from a blue shift of about 100 nm (0.25 eV) of the experimental 750 nm band. In the first excited state (at 1.9 eV), the dipole moment was found to be 1.8 Debye (0.71 au) which with the Born equation leads to $G_{solv} \approx -2.1 \cdot 10^{-5}$ Hartree ($-6 \cdot 10^{-4}$ eV). The ΔG_{solv} (INDO/DRF) = $-2.2 \cdot 10^{-4}$ Hartree ($-6 \cdot 10^{-3}$ eV) is larger than obtained from Eq. (10) by going beyond the point dipole approximation for the charge distribution. For the exciton binding, here approximated as $E_b = -(E_I + E_A)$ where E_I is the ionisation energy and E_A the electron affinity, we get $E_b(\text{vac}) = 3.62$ eV and $E_b(\epsilon = 11, r = 22 \text{ Bohr}) = 2.44$ eV. This is indeed smaller than *in vacuo* but not related like in Eq. (1). However, it leads to an ‘effective’ dielectric constant for the combined system of $3.62/2.44 = 1.48$.

To further improve on the calculation of media effects on the absorption spectrum and the exciton binding energy, we performed some MD calculations with DRF90 on one BO-ADPM molecule surrounded by ten CA molecules, and collected 50 uncorrelated structures from which 50 spectra were calculated. A total of 750 excitation energies were sorted in 3 boxes of width 0.91 eV (the difference of the smallest and largest excitation energy divided by the number of boxes, thus defining the resolution) and adding the oscillator strengths within each box. The results in the boxes were convoluted with gaussians of width 0.27 eV. The resulting spectrum (purple curve in Fig. 5) in the visible region did again not differ significantly from the computed vacuum spectrum. The mean ground state interaction energy with the environment

was $8 \cdot 10^{-4}$ Hartree (0.022 ± 0.016 eV). The exciton binding energy obtained from a single ‘solute/solvent’ configuration is 0.12 Hartree (3.26 eV), *i.e.*, slightly lower than the vacuum exciton binding energy, but even farther from the supposed relation via Eq. (1). Finally, we performed an all QM calculation of the spectrum of BO-ADPM(CA)₁₀ in the solute/solvent configuration mentioned above. Again, no significant differences were obtained: the same spectrum (green curve in Fig. 5), exciton binding energy (0.12 Hartree), and ground state dipole moment (10.01 D) were found, in perfect agreement with the ensemble average of the MD calculations (9.95 D).

Also the dielectric constant of the present system BO-ADPM(CA)₁₀ was calculated following the same procedure as above by applying Eq. (9) with averaged induced dipoles on each atom and averaged radii. We arrived at $\epsilon_{eff} = 1.51$, while the ratio between the averaged binding energy in the cluster and in vacuum gives $\epsilon_{eff} = 1.06$. These results clearly indicate that the screened Coulomb law should not be applied for microscopic situations, and a correct description of the first stages of exciton dissociation can only be given by a microscopic (quantum mechanical) treatment.

Figure 5

6. Conclusions

This study shows that application of the screened Coulomb law modified for dielectrics cannot be used to describe the interaction between charges at the microscopic level. This also holds for the description of exciton dissociation, a vital process in the generation of free charges in OPVs. Thus, it is not obvious that

increasing the dielectric constant of the medium alone is sufficient to yield more efficient OPV devices. Microscopic studies using QM/MM methods are necessary to investigate the effect of the medium on exciton dissociation. This strategy has also been underlined recently in a review of Chiechi *et al.*[34]

Electronic Supplementary Information available Energies and forces between two charges at about 46 Å in Si₄₉₅₀ (Table S1), forces (F/au) between charges at a distance of about 10 Å (the distance between the centres of mass of the acceptor and donor moieties in **1**) in vacuum, in complex **1**, and in **1** ‘solvated’ in slabs of Si and C (Table S2), and coordinates of complex **1** (Å), together with the ‘excitonic’ point charges (p₊ and p₋) that mimick the electron distribution of its first excited state (Table S3).

Acknowledgments

R.W.A.H. acknowledges the Zernike Institute for Advanced Materials (“Dieptestrategie” program) for financial support. This work is part of the research programme of the Foundation of Fundamental Research on Matter (FOM), which is part of the Netherlands Organisation for Scientific Research (NWO). This is a publication of the FOM-focus Group ‘Next Generation Organic Photovoltaics’, participating in the Dutch Institute for Fundamental Energy Research (DIFFER). The work was partially done with computing time at the Dutch National Supercomputer Cartesius (SURFsara, SH-213-13).

References

- [1] L. J. A. Koster, S. E. Shaheen, J. C. Hummelen, *Adv. Energy Mater.*, 2 (2012) 1246.

- [2] T.M. Clarke, J.R. Durrant, *Chem. Rev.*, 110 (2010) 6736.
- [3] S. E. Gledhill, B. Scott, B. A. Gregg, *J. Mater. Res.*, 20 (2005) 3167.
- [4] R. Constanciel, *Theor. Chim. Acta*, 69 (1986) 505.
- [5] J.D. Jackson, *Classical Electrodynamics*, John Wiley & Sons, New York, 1975.
- [6] P.Th. van Duijnen, B.T. Thole, *Biopolymers*, 21 (1982) 1749.
- [7] J.A.C. Rullmann, M.N. Bellido, P.Th. van Duijnen, *J. Mol. Biol.*, 206 (1989) 101.
- [8] A.H. de Vries, P.Th. van Duijnen, A.H. Juffer, *Int. J. Quantum Chem., Quantum Chem.Symp.*, 27 (1993) 451.
- [9] P.Th. van Duijnen, A.H. de Vries, *Int. J. Quantum Chem., Quantum Chem. Symp.*, 29 (1995) 523.
- [10] C. Jarque, A.D. Buckingham, *Chem. Phys. Lett.*, 164 (1989) 485.
- [11] R. Zangi, *J. Chem. Phys.*, 126 (2012) 184501.
- [12] J. Deslippe, M. Dipoppa, D. Prendergast, M.V.O. Moutinho, R.B. Capaz, S.G. Louie, *Nano Lett.*, 9 (2009) 1330.
- [13] J.-W. van der Horst, P.A. Bobbert, M.A.J. Michels, H. Bässler, *J. Chem. Phys.*, 114 (2001) 6950.
- [14] O. Lehtonen, D. Sundholm, T. Vänskä, *Phys. Chem. Chem. Phys.*, 10 (2008) 4535.
- [15] B.A. Gregg, M.C. Hanna, *J. Appl. Phys.*, 93 (2003) 3605.
- [16] B.A. Gregg, S-G. Chen, R.A. Cormier, *Chem. Mater.*, 16 (2004) 4586.
- [17] K. M. Hong, J. Noolandi, *J. Chem. Phys.*, 69 (1978) 5026.
- [18] P. M. Borsenberger, A. I. Ateya, *J. Appl. Phys.*, 50 (1979) 909.
- [19] M. Tachiya, *J. Chem. Phys.*, 89 (1988) 6929.

- [20] V. D. Mihailetschi, L. J. A. Koster, J. C. Hummelen, P.W.M. Blom, *Phys. Rev. Lett.*, 93 (2004) 216601.
- [21] V.D. Mihailetschi, L.J.A.Koster, P.W.M. Blom, C. Melzer, B. de Boer, J.K.J. van Duren, R.A.J. Janssen, *Adv. Funct. Mater.*, 15 (2005) 795.
- [22] M. Wojcik, M. Tachiya, *Rad. Phys. Chem.*, 74 (2005) 132.
- [23] M. Lenes, F. B. Kooistra, J. C. Hummelen, I. Van Severen, L. Lutsen, D. Vanderzande, T. J. Cleij, P. W. M. Blom, *J. Appl. Phys.*, 104 (2008) 114517.
- [24] M. Swart, P.Th. van Duijnen, *Mol. Simul.*, 32 (2006) 471.
- [25] P.Th. van Duijnen, M. Swart, *J. Phys. Chem. C*, 114 (2010) 20547.
- [26] B.T. Thole, *Chem. Phys. Lett.*, 59 (1981) 341.
- [27] P.Th. van Duijnen, M. Swart, *J. Phys. Chem. A*, 102 (1998) 2399.
- [28] M. Swart, P.Th. van Duijnen, J.G. Snijders, *J. Mol. Struct. (Theochem)*, 458 (1999) 11.
- [29] C. Pouchan, D. Begue, D.Y. Zhang, *J. Chem. Phys.*, 121 (2004) 4628.
- [30] M.C. Zerner, *Semi Empirical Molecular Orbital Methods*, in: K.B. Lipkowitz, D.B.N. Boyd (Eds.) *Reviews of Computational Chemistry*, VCH, New York, 1991, pp. 313.
- [31] N.L. Allinger, Y.H. Yuh, J.-H. Lii, *J. Am. Chem. Soc.*, 111 (1989) 8551.
- [32] M.F. Guest, I.J. Bush, H.J.J. van Dam, P. Sherwood, J.M.H.Thomas, J.H. van Lenthe, R.W.A. Havenith, J. Kendrick, *Mol. Phys.*, 103 (2005) 719.
- [33] S.Y. Leblebici, T.L. Chen, P. Olada-Velasco, W. Yang, B. Ma, *ACS Appl. Mater. Interfaces*, 5 (2013) 10105.
- [34] R.C. Chiechi, R.W.A. Havenith, J.C. Hummelen, L.J.A. Koster, M.A. Loi, *Mater. Today*, 16 (2013) 281.

Table 1. Forces (F/au) between charged atoms (1.0 au) in Si₄₉₅₀, about 46 Å apart, by finite differences F_{elst} = electrostatic (unscreened) force. Since the remaining atoms are neutral and the distance between the charged atoms is so large that no screening occurs, $F_{\text{elst}} = F_{\text{vac}}$. F_{ind} = force due to induction, F_{total} = total force, $\epsilon_{\text{eff}} = F_{\text{vac}}/F_{\text{total}}$. For details, see Table S1.

	charges +/-	+/+
F_{elst}	$-0.132 \cdot 10^{-3}$	$0.132 \cdot 10^{-3}$
F_{ind}	$-0.357 \cdot 10^{-3}$	$-0.502 \cdot 10^{-3}$
F_{total}	$-0.489 \cdot 10^{-3}$	$-0.370 \cdot 10^{-3}$
ϵ_{eff}	0.27	-0.36

Table 2. Forces (F/au) between charges at a distance of about 10 Å (the distance between the centres of mass of the acceptor and donor moieties in **1**) in vacuum, in complex **1**, and in **1** ‘solvated’ in slabs of Si and C. For details, see Table S2.

Charges	Environment	Electrostatic	Induction	Total	ϵ_{eff}
+/-	vacuum	$-2.86 \cdot 10^{-3}$			1
+/-	1	$1.35 \cdot 10^{-3}$	$1.18 \cdot 10^{-3}$	$2.53 \cdot 10^{-3}$	-
+/-	1 in C ₄₉₅₀	$1.35 \cdot 10^{-3}$	$4.67 \cdot 10^{-3}$	$6.03 \cdot 10^{-3}$	-
+/-	1 in Si ₄₉₅₀	$1.35 \cdot 10^{-3}$	$5.10 \cdot 10^{-3}$	$6.45 \cdot 10^{-3}$	-
+/-	C ₄₉₅₀	$-2.67 \cdot 10^{-3}$	$2.77 \cdot 10^{-3}$	$9.63 \cdot 10^{-5}$	-30
+/+	C ₄₉₅₀	$2.67 \cdot 10^{-3}$	$-1.04 \cdot 10^{-3}$	$1.67 \cdot 10^{-3}$	-2
+/-	Si ₄₉₅₀	$-2.67 \cdot 10^{-3}$	$1.00 \cdot 10^{-3}$	$-1.67 \cdot 10^{-3}$	2
+/+	Si ₄₉₅₀	$2.67 \cdot 10^{-3}$	$-3.42 \cdot 10^{-3}$	$-7.47 \cdot 10^{-4}$	4

Figure 1. Effective atomic polarisability of C and Si in 4950-clusters with diamond structure as a function of the distance to the centre.

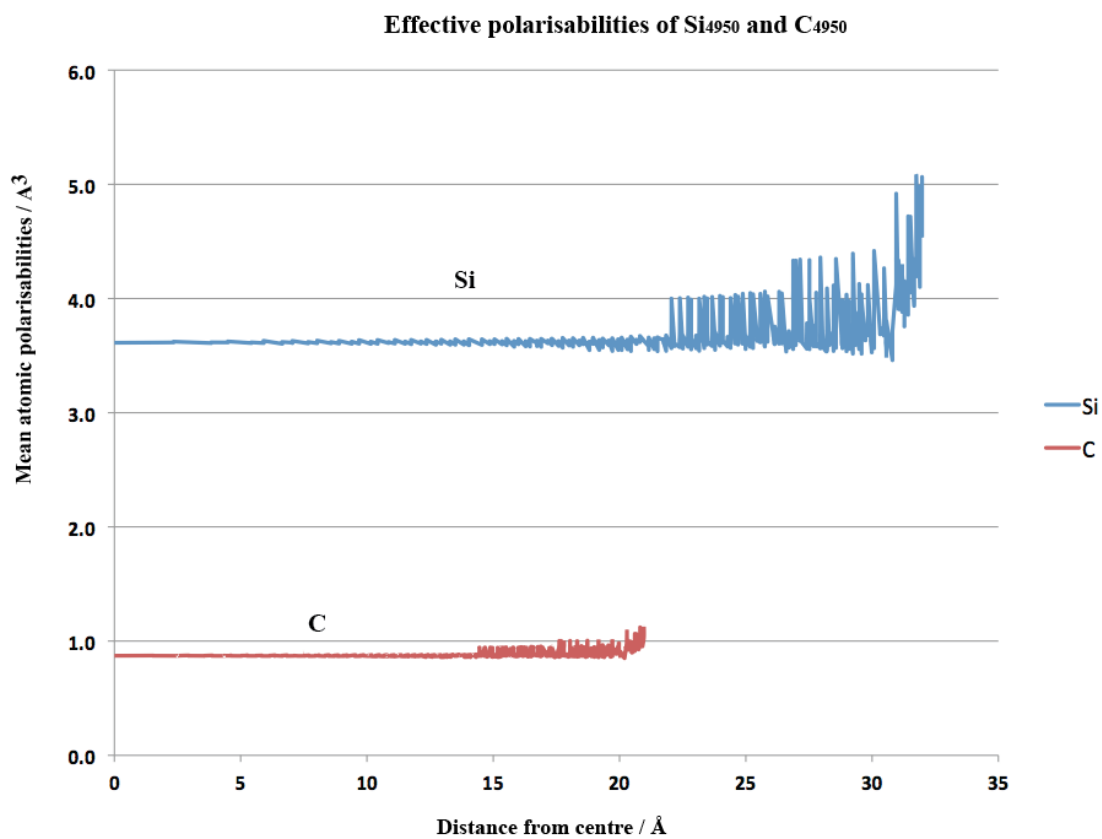


Figure 2. The donor-acceptor complex **1**. The ‘hydrogen atoms’ in the centres of Acceptor and Donor represent the (dressed) point charges mimicking an exciton.

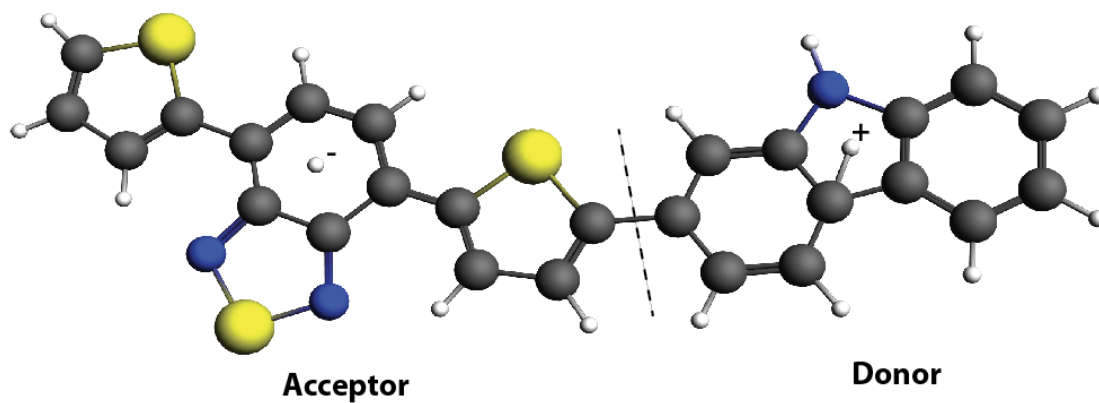


Figure 3. 1 'solvated' in ~ 4950 C- or Si-atoms.

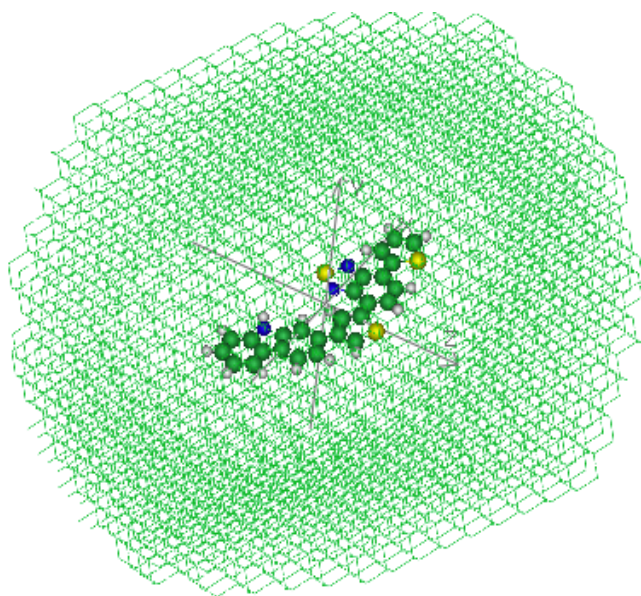


Figure 4. The force (au) between a plus and a minus charge as a function of their distance (\AA) in nonane (**2**), 1-methoxy-2-(2-methoxyethoxy)ethane (**3**), and 1,8-diiodooctane (**4**), respectively. In a), the molecules are treated at the HF/6-31G level, in b) the molecules are treated with the DRF approach. For comparison, the force in vacuum is also plotted.

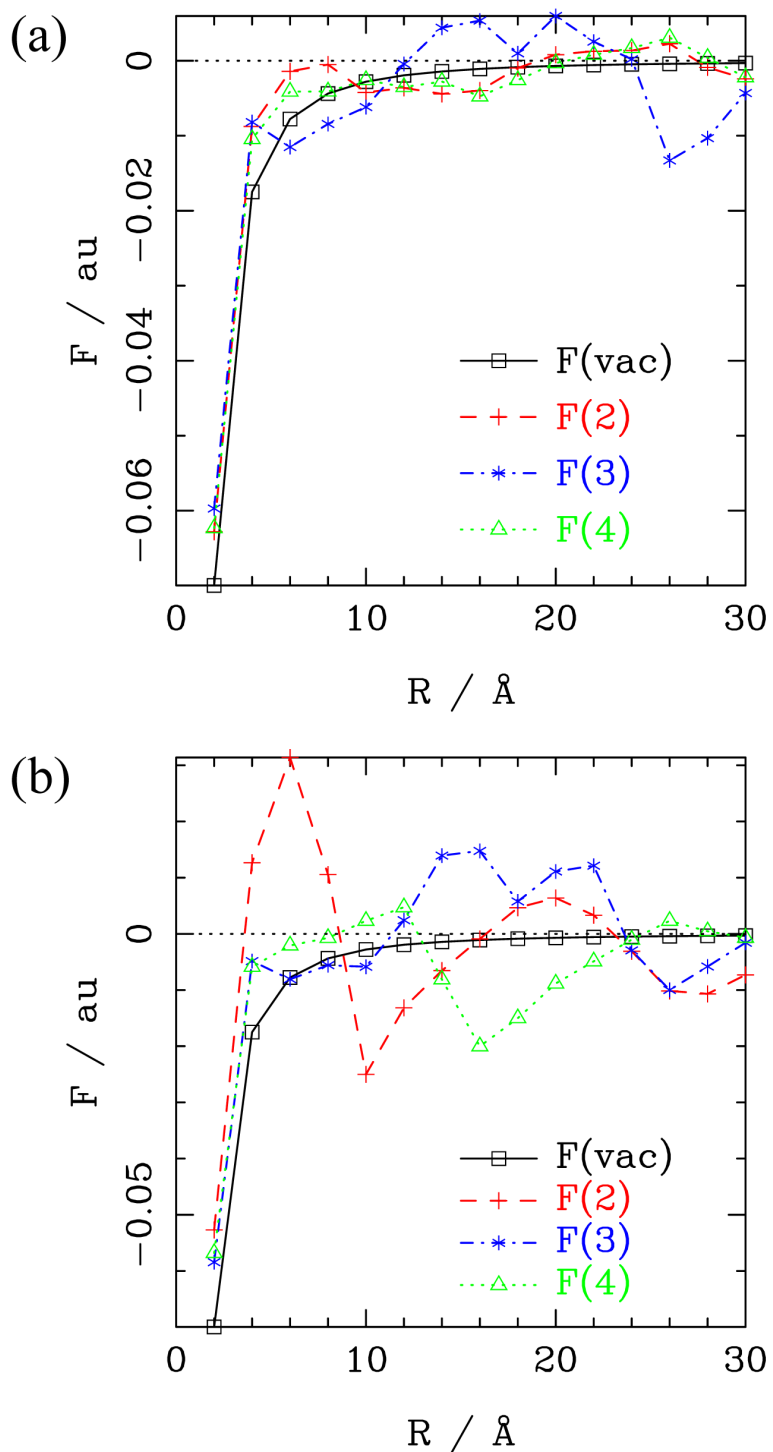


Figure 5. Absorption spectra of BO-ADPM. The blue curve shows the spectrum of BO-ADPM *in vacuo*, the red curve shows the spectrum of BO-ADPM in a spherical cavity with $r = 22$ Bohr embedded in a dielectric continuum with $\epsilon = 11$, the purple one shows the spectrum of 50 uncorrelated structures obtained by MD calculations with DRF90 on one BO-ADPM molecule surrounded by ten CA molecules, and the green one shows the spectrum obtained by an all QM calculation of the spectrum of BO-ADPM(CA)₁₀ in the solute/solvent configuration mentioned in the main text.

